GEOLOGY | THE GEOLOGICAL SOCIETY OF AMERICA®

https://doi.org/10.1130/G45480.1

Manuscript received 13 August 2018
Revised manuscript received 30 November 2018
Manuscript accepted 19 December 2018

Synchronous cooling and decline in monsoonal rainfall in northeastern Tibet during the fall into the Oligocene icehouse

M. Page[1], A. Licht[1], G. Dupont-Nivet[2,3,4], N. Meijer[2], N. Barbolini[5], C. Hoorn[5], A. Schauer[1], K. Huntington[1], D. Bajnai[6], J. Fiebig[6], A. Mulch[6,7], and Z. Guo[4]

[1]Department of Earth and Space Sciences, University of Washington, Seattle, Washington 98195, USA
[2]Universität Potsdam, Institute of Earth and Environmental Science, 14476 Potsdam, Germany
[3]Géosciences Rennes, UMR CNRS 6118, Université de Rennes, CS 74205, 35042 Rennes, France
[4]Key Laboratory of Orogenic Belts and Crustal Evolution, Peking University, Beijing 100871, China
[5]Department of Ecosystem and Landscape Dynamics, Institute for Biodiversity and Ecosystem Dynamics, University of Amsterdam, Amsterdam 1098 XH, Netherlands
[6]Institute of Geosciences, Goethe University, 60438 Frankfurt am Main, Germany
[7]Senckenberg Biodiversity and Climate Research Centre, 60325 Frankfurt am Main, Germany

ABSTRACT

The fall into the Oligocene icehouse is marked by a steady decline in global temperature with punctuated cooling at the Eocene-Oligocene transition, both of which are well documented in the marine realm. However, the chronology and mechanisms of cooling on land remain unclear. Here, we use clumped isotope thermometry on northeastern Tibetan continental carbonates to reconstruct a detailed Paleogene surface temperature record for the Asian continental interior, and correlate this to an enhanced pollen data set. Our results show two successive dramatic (>9 °C) temperature drops, at 37 Ma and at 33.5 Ma. These large-magnitude decreases in continental temperatures can only be explained by a combination of both regional cooling and shifts of the rainy season to cooler months, which we interpret to reflect a decline of monsoonal intensity. Our results suggest that the response of Asian surface temperatures and monsoonal rainfall to the steady decline of atmospheric CO_2 and global temperature through the late Eocene was nonlinear and occurred in two steps separated by a period of climatic instability. Our results support the onset of the Antarctic Circumpolar Current coeval to the Oligocene isotope event 1 (Oi-1) glaciation at 33.5 Ma, reshaping the distribution of surface heat worldwide; however, the origin of the 37 Ma cooling event remains less clear.

INTRODUCTION

The Eocene-Oligocene transition (EOT) from the greenhouse warm period of the Eocene to the icehouse conditions of the Oligocene was one of the most pronounced periods of global cooling during the Cenozoic (Pagani et al., 2011).

Marine geological records have shown that atmospheric CO_2 levels and global temperature declined steadily during the late Eocene (Pearson and Palmer, 2000; Eldrett et al., 2009; Pearson et al., 2009). This long-term decrease eventually prompted the sudden development of expanded Antarctic ice sheets, controlled by favorable orbital conditions and a CO_2 threshold (DeConto and Pollard, 2003; Pearson et al., 2009). The growth of these ice sheets is recorded by two consecutive shifts in marine $\delta^{18}O$ values, at the EOT isotope event 1 (EOT-1) at 34.0 Ma and again at the Oligocene isotope event 1 (Oi-1) glaciation at ca. 33.5 Ma (Katz et al., 2008; Miller et al., 2009). Each of these events resulted in ~5 °C of cooling at high latitudes and a total drop in sea level of ~100 m (Miller et al., 2009; Liu et al. 2009).

Although marine records of Paleogene climate have been well studied, few records exist that correlate marine temperature to the surface temperatures of the Asian continental interior. Pollen and macrofossil assemblages from across China corroborate a long-term temperature decrease and trend toward harsher winters through the late Eocene (Quan et al., 2012) with a marked increase in regional aridity (Dupont-Nivet et al., 2007) that has been related to a proposed coeval decline of summer monsoonal intensity (Licht et al., 2014). However, the paucity of well-dated macrofossil assemblages from Asia covering the EOT have hindered efforts to better document these changes in continental climate.

Clumped isotope approaches to paleotemperature reconstructions are particularly relevant in deep time because they are less sensitive to changes in biomes and ecosystems. However, only a few studies have tried to address continental cooling through the EOT using clumped isotope thermometry. Fan et al. (2017) inferred an ~8 °C decrease in North American mean annual temperature recorded in vadose carbonate cements. In contrast, clumped isotope thermometry applied to aragonite shells in England suggests that inland water bodies experienced 4–6 °C of cooling, similar to what is recorded in North Atlantic marine sediment (Hren et al., 2013).

Here, we use clumped isotope thermometry on vadose-grown carbonates from the Xining Basin, northeastern Tibet (Fig. 1), to reconstruct the first Paleogene surface temperature record for the Asian interior covering the fall into the icehouse, which is complemented by an updated and expanded palynological record now covering the EOT.

XINING BASIN CONTEXT

The Xining Basin is part of a system of basins at the northeastern margin of the Tibetan Plateau (Dai et al., 2006). Xining's modern climate is semiarid, and monthly daily temperature averages range from –7.4 °C in January to 17.3 °C in July with an annual mean of 6.1 °C.

CITATION: Page, M., et al., 2019, Synchronous cooling and decline in monsoonal rainfall in northeastern Tibet during the fall into the Oligocene icehouse: Geology, https://doi.org/10.1130/G45480.1.

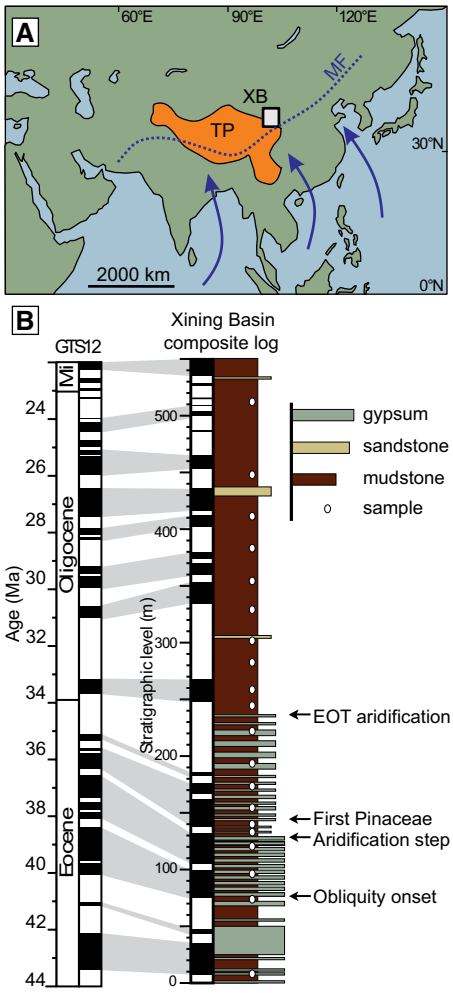

Figure 1. A: Map of Asia showing location of Xining Basin (XB), Tibetan Plateau (TP), and summer monsoonal front (MF), with summer wind directions shown by blue arrows. B: Regional stratigraphy of Xining Basin with stratigraphic location of our samples (age and correlations from Dai et al., 2006; Abels et al., 2011; Bosboom et al., 2014). GTS12—Geological Time Scale 2012; EOT—Eocene-Oligocene transition.

The modern average annual rainfall of 373 mm is controlled by monsoonal weather patterns, with 70% of precipitation occurring during the summer and the remaining part occurring during the winter from westerly-derived moisture (Hoorn et al., 2012).

Magnetostratigraphic dating indicates relatively low and continuous sediment accumulation rates in the Xining Basin, from its 55–50 Ma formation to its partitioning and uplift ca. 15 Ma (Dai et al., 2006). Paleogene units are dominated by red mudstone with carbonate cement, alternating with cyclic gypsum deposits formed from the evaporation of playa lakes (Abels et al., 2011). The abundance of gypsum decreases at 37.1 Ma, and the gypsum deposits largely disappear by 34 Ma, which has been interpreted to represent long-term shrinking of the playa system in response to successive decreases in moisture availability (Fig. 2; Dupont-Nivet et al., 2007; Abels et al., 2011). The first decrease in gypsum abundance at 37.1 Ma is shortly followed by an upswing (>10% of the palynomorph sum) in Pinaceae pollen coming from the nearby mountain ranges at 36.5 Ma, indicating sudden cooling a few million years before the EOT (Hoorn et al., 2012).

METHODS

Samples of carbonate-bearing mudstones were collected from the Xining Basin along three previously dated sections covering the time interval from the middle Eocene to the earliest Miocene, at the localities of Shuiwan (Abels et al., 2011), Tiefo (Bosboom et al., 2014), and Xieja (Dai et al., 2006). Ages were determined from the available paleomagnetic and cyclostratigraphic data, with an estimated uncertainty of ~0.1 m.y. per sample. Nineteen (19) test samples were prepared in thin section and examined using cathodoluminescence and polarized-light microscopy to evaluate the origin and potential for diagenesis of carbonates. Carbonates were identified as vadose-grown cements precipitated from soil water and did not show any evidence for subsequent diagenetic alteration (see the GSA Data Repository[1]). Vadose-grown cements can precipitate from soil water or shallow groundwater and commonly form in the same growth season as soil carbonates (Quade and Roe, 1999; Fan et al., 2017).

Clumped isotope thermometry uses the concentration of ^{13}C-^{18}O bonds in carbonates as a proxy for the temperature of formation of the carbonate. $T_{\Delta47}$ is the clumped isotope–derived temperature, which is calculated from the Δ_{47} values (the amount of CO_2 isotopologue with a mass 47 relative to the amount expected if carbon and oxygen isotopes were stochastically distributed) using a formula derived from calibration experiments (e.g., Kelson et al., 2017). In soils and vadose cements, clumped isotope thermometry is a direct indicator of carbonate growth temperature. This method can be susceptible to seasonal biases; changes in carbonate $T_{\Delta47}$ can be thus interpreted in terms of changing temperature for a given region and/or of change in carbonate growth season (Peters et al., 2013; Fan et al., 2017).

Twenty (20) mudstone samples were analyzed for Δ_{47} with three to five replicates each at the University of Washington, Seattle, USA (following Kelson et al., 2017), and at Goethe University, Frankfurt, Germany (following Bajnai et al., 2018). The resulting Δ_{47} values were converted to clumped isotope temperatures following Kelson et al. (2017). Age, location of samples, and detailed results for samples and standards are given in Table DR1 in the Data Repository.

Five (5) new palynological samples were collected from gypsum beds preserving lacustrine laminations of greenish-gray mud; samples were prepared by Palynological Laboratory Services (Anglesey, UK), and examined at the University of Amsterdam (Netherlands). Two samples through the EOT interval proved productive and were added to the existing pollen data set of Hoorn et al. (2012) updated to the Geological Time Scale 2012 (Gradstein et al., 2012).

RESULTS

Xining carbonate $T_{\Delta47}$ values are in the range of Earth-surface temperatures (<40 °C) with abrupt changes coeval with independently documented periods of climatic change (Fig. 2).

From 43.5 to 37.5 Ma, $T_{\Delta47}$ values are relatively constant at ~29 °C, 12 °C warmer than today's summer air temperatures in the Xining Basin. The palynological record indicates that steppe-desert (xerophytic and halophytic) taxa dominated the landscape, with a lesser component of broad-leaved forest, and few to no conifers (Fig. DR1). $T_{\Delta47}$ values abruptly decrease between 37.7 and 37.0 Ma, and stay at a low of ~20 °C until 35 Ma. This abrupt decrease coincides with the first aridification step in the section, which is marked by a significant decrease in gypsum bed thickness corresponding with a decline of the playa lake system (Abels et al., 2011), and slightly precedes the sudden increase in Pinaceae pollen in the basin, which likely originated from the surrounding highlands (Hoorn et al., 2012; Fig. 2).

From 35 to 33.7 Ma, $T_{\Delta47}$ values oscillate between warm and cold conditions, with vegetation also displaying variability (Fig. 2; Fig. DR1). $T_{\Delta47}$ values eventually drop dramatically starting between 33.7 and 33.3 Ma, decreasing by ~20 °C from 35 ± 6 °C to 15 ± 4 °C at 31.3 Ma (1σ). This second temperature drop is reflected by a pronounced increase in the abundance and diversity of Pinaceae (Fig. 2) and the disappearance of frost-intolerant broad-leaved taxa (Fig. DR1). Temperature rises to between 20 °C and 25 °C during the last 5 m.y. of our record, which ends in the latest Oligocene.

DISCUSSION

The $T_{\Delta47}$ results for all of our samples are within a reasonable range for Earth-surface temperatures, which is consistent with vadose carbonates that have not undergone later deep diagenesis. Interestingly, our $T_{\Delta47}$ values are 5–15 °C higher than modern-day summer air temperature, and get close to modern values only during the early Oligocene. The range of Eocene $T_{\Delta47}$ values (20–35 °C) is very similar to late Eocene summer temperature of coastal China (~25 °C) estimated from pollen assemblages (Quan et al.,

[1]GSA Data Repository item 2019069, evaluation of the origin and potential for diagenesis of our carbonate samples, complete isotope data (Table DR1), and pollen data (Figure DR1), is available online at http://www.geosociety.org/datarepository/2019/, or on request from editing@geosociety.org.

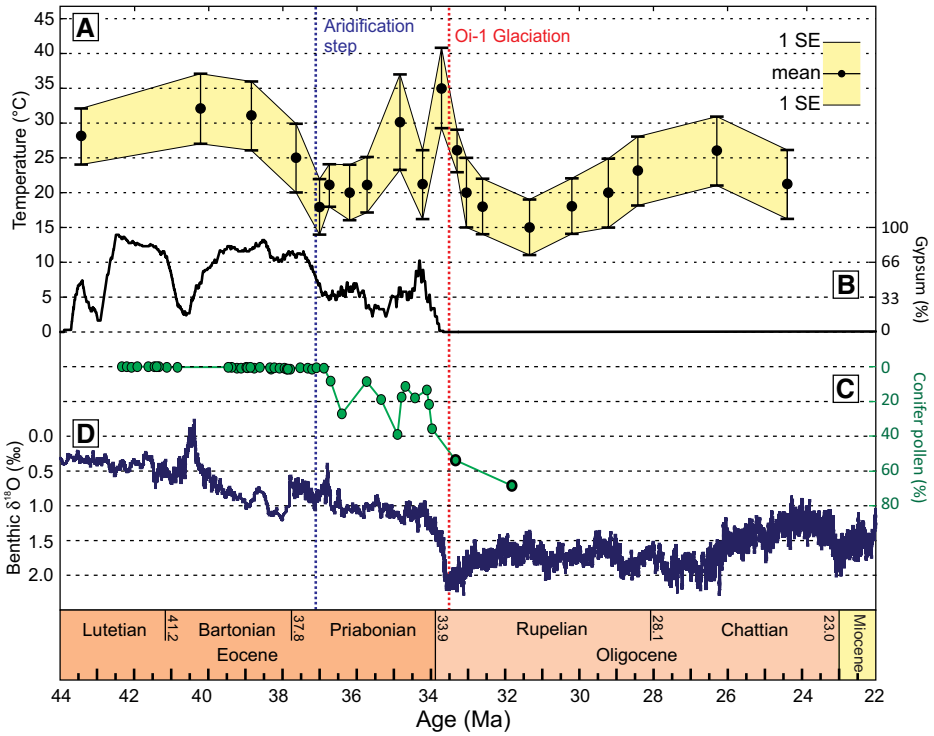

Figure 2. Clumped isotope temperatures ($T_{\Delta47}$) from middle Eocene to lower Miocene in Xining Basin, northeastern Tibet (A; error bars = 1 standard error [SE]), compared with gypsum content (B; 10 m moving average on gypsum occurrence in sections; Abels et al., 2011), relative proportion of conifer pollen as percentage of total terrestrial pollen (C; new samples in thick black circles), and evolution of benthic foraminiferal $\delta^{18}O$ (D; after Gradstein et al., 2012). Oi-1—Oligocene isotope event 1.

2012), consistent with the Xining Basin being at a lower elevation during the Eocene.

Our results highlight two episodes of significant decrease in carbonate growth temperature: the first at 37 Ma (~9 °C decrease) and the second starting between 33.7 and 33.5 Ma reaching a minimum temperature at 31.3 Ma (~20 °C drop in total), with a period of recovery between the two events. The second drop in temperature appears coeval with the onset of Oi-1 glaciation at 33.5 Ma (Miller et al., 2009). These $T_{\Delta47}$ changes are too sudden to be driven by changes in basin altitude, and the synchronicity of the second drop with the Oi-1 glaciation renders surface uplift unlikely as a main cause for cooling.

The magnitude of the second cooling event is significantly larger than previously proposed for the EOT (Hren et al., 2013; Fan et al., 2017) and appears too large for a shift in regional temperature only. Development of a forested vegetation cover could have decreased local ground heating (Quade et al., 2013) and could explain part of the observed cooling, but Xining red mudstones were deposited on the dry, distal part of past playa systems, areas commonly unvegetated or only sparsely covered by shrubs (Abels et al., 2011). Rather, our results are best explained by a combination of decreasing regional temperature coupled with a shift in the season of carbonate growth to cooler months. Carbonates precipitated from soil water, including nodules and vadose cements, grow when the ground dries after seasonal rainfall. This phenomenon is favored during warmer seasons because high soil temperatures decrease calcite solubility, and evaporation and plant evapotranspiration increase calcium activity in the soil water (e.g., Breecker et al., 2009). In Tibet today, carbonate growth occurs mostly during the summer monsoon, when both rainfall and temperature are at their highest (Quade et al., 2013). In Xining, a longer and more-intense monsoonal season would shift the season of carbonate formation into the late summer and fall. By contrast, a shorter and less-intense monsoonal season would increase the relative contribution of winter, westerly-derived moisture to the annual rainfall budget. The proportion of carbonate growing in spring, when the soils start to dry out after the winter rains, would start becoming significant, shifting the average carbonate growth temperature to colder values, closer to mean annual temperatures. Less-intense and shorter monsoons during both cooling events is also more consistent with the observed decrease and final disappearance of gypsum beds, reflecting water table drops in the Xining Basin in response to decreasing moisture input (Dupont-Nivet et al., 2007). Therefore, the apparently dramatic temperature drop at 33.5 Ma, and possibly at 37 Ma, is best explained by coeval decrease in regional temperature and monsoonal rainfall.

Fluctuations of Pinaceae over the past 100 m.y. are strongly correlated with temperature (Brodribb et al., 2012), but a concurrent shift of moisture availability to the cooler months would further favor the ecological dominance of conifers over the EOT. Unlike deciduous taxa, evergreen conifers can grow during the winter, and their small, needle-like waxy leaves also prevent water loss in the dry summers, which would have provided a dual advantage as monsoonal rainfall declined (Su et al., 2013).

Although it is impossible to decipher the exact contribution of cooling versus change of carbonate growth season in the $T_{\Delta47}$ values, a shift from July to April for carbonate growth today would result in an apparent ~9 °C drop in Xining (https://en.climate-data.org). Such a shift in growth season would require a coeval ~11 °C cooling of surface temperatures through the EOT to explain the ~20 °C drop, which is close to the surface cooling observed in North America (~8 °C; Fan et al., 2017).

The synchronicity of cooling and drop of monsoonal intensity is not surprising, as continental summer temperatures drive moist static energy, which directly controls monsoonal intensity at the continental scale (Roe et al., 2016). Previous climate simulations have suggested up to a twofold decrease of summer rainfall in Xining through the fall into the icehouse (Licht et al., 2014). This first cooling event at ca. 37 Ma is particularly intriguing because it is virtually undocumented on other continents. As with the later cooling event at 33.5 Ma, we interpret this decrease in $T_{\Delta47}$ to indicate a period of cooling, yet of lesser magnitude, that triggered a shift in rainfall to earlier months. This drop could reflect a first major glaciation in the late Eocene, corroborating independent evidence for Antarctic ice-sheet spreading around that time (Carter et al., 2017). This first cooling event is followed by a period from 35 to 33.5 Ma during which clumped isotope temperatures, gypsum thickness, and conifer pollen content appear uncorrelated (Fig. 2). Note that our three proxies do not record exactly the same sampling intervals and do not derive from the same beds (i.e., carbonates are from red mudstone and pollen is from lacustrine laminations within gypsum beds). These three different records may thus reflect slightly different vegetation cover, which determines the amount of solar radiation to shallow ground. It is also possible that the climate could have changed erratically and so rapidly during the period that our proxies do not record the same trends. Both temperature and summer monsoonal intensity were eventually significantly affected by the Oi-1 glaciation, with $T_{\Delta47}$ reaching its lowest values. The climatic system started to slowly recover in the mid-Oligocene, but carbonate growth temperatures did not return to pre–37 Ma values.

The interconnection between ice-sheet expansion, cooling in the Asian interior, and

consequent decline of Asian monsoonal intensity is not straightforward. Studies of marine sediment and climate simulations have proposed a partial redistribution of surface heat at the global scale following the Oi-1 glaciation (Katz et al., 2011). The onset of the Antarctic Circumpolar Current would have increased the northward transport of cold Antarctic water (Miller et al. 2009), which could have significantly impacted surface temperature in the Northern Hemisphere, lowered atmospheric moist static energy at the continental scale in Asia, and provoked the decline of monsoonal intensity, thus providing a possible mechanism for the changes observed at our study site.

CONCLUSION

Our clumped isotope results indicate two temperature drops, the first step occurring at 37 Ma and the second at 33.5 during the Oi-1 glaciation, which are too large to be explained by regional cooling alone, and are interpreted as a combination of cooling and carbonate growth season shift to cooler months in response to declining monsoonal intensity. Our results suggest that the response of Asian temperatures and monsoonal rainfall to the steady decline of atmospheric CO_2 and global temperature through the late Eocene was nonlinear, occurring in two steps separated by a period of climatic instability. Surface temperatures and monsoonal intensity declined synchronously, corroborating the strong influence of regional surface temperatures on summer monsoonal intensity. Our results support an onset of the Antarctic Circumpolar Current coeval to the Oi-1 glaciation, reshaping the distribution of surface heat at the global scale and consequently weakening monsoonal intensity. The origin of the 37 Ma cooling event remains to be investigated.

ACKNOWLEDGEMENTS

This study was financially supported by the University of Washington. Dupont-Nivet, Meijer, and Barbolini acknowledge funding from European Research Council consolidator grant MAGIC 649081. Huntington acknowledges funding from U.S. National Science Foundation grants EAR-1252064 and EAR-1156134. We thank L. Burgener, J. Kelson, and M. Strecker for prolific discussions and assistance in the lab, and P. Bartlett for editorial assistance. We thank Carmala Garzione, Nathan Sheldon, Miquela Ingalls, and two anonymous reviewers for comments that improved this work.

REFERENCES CITED

Abels, H.A., Dupont-Nivet, G., Xiao, G., Bosboom, R., and Krijgsman, W., 2011, Step-wise change of Asian interior climate preceding the Eocene–Oligocene Transition (EOT): Palaeogeography, Palaeoclimatology, Palaeoecology, v. 299, p. 399–412, https://doi.org/10.1016/j.palaeo.2010.11.028.

Bajnai, D., Fiebig, J., Tomašových, A., Garcia, S.M., Rollion-Bard, C., Raddatz, J., Löffler, N., Primo-Ramos, C., and Brand, U., 2018, Assessing kinetic fractionation in brachiopod calcite using clumped isotopes: Scientific Reports, v. 8, 533, https://doi.org/10.1038/s41598-017-17353-7.

Bosboom, R.E., Abels, H.A., Hoorn, C., van den Berg, B.C., Guo, Z., and Dupont-Nivet, G., 2014, Aridification in continental Asia after the Middle Eocene Climatic Optimum (MECO): Earth and Planetary Science Letters, v. 389, p. 34–42, https://doi.org/10.1016/j.epsl.2013.12.014.

Breecker, D.O., Sharp, Z.D., and McFadden, L.D., 2009, Seasonal bias in the formation and stable isotopic composition of pedogenic carbonate in modern soils from central New Mexico, USA: Geological Society of America Bulletin, v. 121, p. 630–640, https://doi.org/10.1130/B26413.1.

Brodribb, T.J., Pittermann, J., and Coomes, D.A., 2012, Elegance versus speed: Examining the competition between conifer and angiosperm trees: International Journal of Plant Sciences, v. 173, p. 673–694, https://doi.org/10.1086/666005.

Carter, A., Riley, T.R., Hillenbrand, C.-D., and Rittner, M., 2017, Widespread Antarctic glaciation during the late Eocene: Earth and Planetary Science Letters, v. 458, p. 49–57, https://doi.org/10.1016/j.epsl.2016.10.045.

Dai, S., Fang, X., Dupont-Nivet, G., Song, C., Gao, J., Krijgsman, W., Langereis, C., and Zhang, W., 2006, Magnetostratigraphy of Cenozoic sediments from the Xining Basin: Tectonic implications for the northeastern Tibetan Plateau: Journal of Geophysical Research, v. 111, B11102, https://doi.org/10.1029/2005JB004187.

DeConto, R.M., and Pollard, D., 2003, Rapid Cenozoic glaciation of Antarctica induced by declining atmospheric CO_2: Nature, v. 421, p. 245–249, https://doi.org/10.1038/nature01290.

Dupont-Nivet, G., Krijgsman, W., Langereis, C.G., Abels, H.A., Dai, S., and Fang, X., 2007, Tibetan plateau aridification linked to global cooling at the Eocene–Oligocene transition: Nature, v. 445, p. 635–638, https://doi.org/10.1038/nature05516.

Eldrett, J.S., Greenwood, D.R., Harding, I.C., and Huber, M., 2009, Increased seasonality through the Eocene to Oligocene transition in northern high latitudes: Nature, v. 459, p. 969–973, https://doi.org/10.1038/nature08069.

Fan, M., Ayyash, S.A., Tripati, A., Passey, B.H., and Griffith, E.M., 2017, Terrestrial cooling and changes in hydroclimate in the continental interior of the United States across the Eocene-Oligocene boundary: Geological Society of America Bulletin, v. 130, p. 1073–1084, https://doi.org/10.1130/B31732.1.

Gradstein, F.M., Ogg, J.G., Schmitz, M., and Ogg, G., eds., 2012, The Geological Time Scale 2012: Amsterdam, Elsevier, 1144 p.

Hoorn, C., Straathof, J., Abels, H.A., Xu, Y., Utescher, T., and Dupont-Nivet, G., 2012, A late Eocene palynological record of climate change and Tibetan Plateau uplift (Xining Basin, China): Palaeogeography, Palaeoclimatology, Palaeoecology, v. 344–345, p. 16–38, https://doi.org/10.1016/j.palaeo.2012.05.011.

Hren, M.T., Sheldon, N.D., Grimes, S.T., Collinson, M.E., Hooker, J.J., Bugler, M., and Lohmann, K.C., 2013, Terrestrial cooling in Northern Europe during the Eocene–Oligocene transition: Proceedings of the National Academy of Sciences of the United States of America, v. 110, p. 7562–7567, https://doi.org/10.1073/pnas.1210930110.

Katz, M.E., Miller, K.G., Wright, J.D., Wade, B.S., Browning, J.V., Cramer, B.S., and Rosenthal, Y., 2008, Stepwise transition from the Eocene greenhouse to the Oligocene icehouse: Nature Geoscience, v. 1, p. 329–334, https://doi.org/10.1038/ngeo179.

Katz, M.E., Cramer, B.S., Toggweiler, J.R., Esmay, G., Liu, C., Miller, K.G., Rosenthal, Y., Wade, B.S., and Wright, J.D., 2011, Impact of Antarctic Circumpolar Current development on late Paleogene ocean structure: Science, v. 332, p. 1076–1079, https://doi.org/10.1126/science.1202122.

Kelson, J.R., Huntington, K.W., Schauer, A.J., Saenger, C., and Lechler, A.R., 2017, Toward a universal carbonate clumped isotope calibration: Diverse synthesis and preparatory methods suggest a single temperature relationship: Geochimica et Cosmochimica Acta, v. 197, p. 104–131, https://doi.org/10.1016/j.gca.2016.10.010.

Licht, A., et al., 2014, Asian monsoons in a late Eocene greenhouse world: Nature, v. 513, p. 501–506, https://doi.org/10.1038/nature13704.

Liu, Z., Pagani, M., Zinniker, D., DeConto, R., Huber, M., Brinkhuis, H., Shah, S.R., Leckie, R.M., and Pearson, A., 2009, Global cooling during the Eocene-Oligocene climate transition: Science, v. 323, p. 1187–1190, https://doi.org/10.1126/science.1166368.

Miller, K.G., Wright, J.D., Katz, M.E., Wade, B.S., Browning, J.V., Cramer, B.S., and Rosenthal, Y., 2009, Climate threshold at the Eocene-Oligocene transition: Antarctic ice sheet influence on ocean circulation, *in* Koeberl, C., and Montanari, A., eds., The Late Eocene Earth: Hothouse, Icehouse, and Impacts: Geological Society of America Special Publication 452, p. 169–178, https://doi.org/10.1130/2009.2452(11).

Pagani, M., Huber, M., Liu, Z., Bohaty, S.M., Henderiks, J., Sijp, W., Krishnan, S., and DeConto, R.M., 2011, The role of carbon dioxide during the onset of Antarctic glaciation: Science, v. 334, p. 1261–1264, https://doi.org/10.1126/science.1203909.

Pearson, P.N., and Palmer, M.R., 2000, Atmospheric carbon dioxide concentrations over the past 60 million years: Nature, v. 406, p. 695–699, https://doi.org/10.1038/35021000.

Pearson, P.N., Gavin, L.F., and Wade, B.S., 2009, Atmospheric carbon dioxide through the Eocene–Oligocene climate transition: Nature, v. 461, p. 1110–1113, https://doi.org/10.1038/nature08447.

Peters, N.A., Huntington, K.W., and Hoke, G.D., 2013, Hot or not? Impact of seasonally variable soil carbonate formation on paleotemperature and O-isotope records from clumped isotope thermometry: Earth and Planetary Science Letters, v. 361, p. 208–218, https://doi.org/10.1016/j.epsl.2012.10.024.

Quade, J., and Roe, L.J., 1999, The stable-isotope composition of early ground-water cements from sandstone in paleoecological reconstruction: Journal of Sedimentary Research, v. 69, p. 667–674, https://doi.org/10.2110/jsr.69.667.

Quade, J., Eiler, J., Daeron, M., and Achyuthan, H., 2013, The clumped isotope geothermometer in soil and paleosol carbonate: Geochimica et Cosmochimica Acta, v. 105, p. 92–107, https://doi.org/10.1016/j.gca.2012.11.031.

Quan, C., Liu, Y.-S.C., and Utescher, T., 2012, Paleogene temperature gradient, seasonal variation and climate evolution of northeast China: Palaeogeography, Palaeoclimatology, Palaeoecology, v. 313–314, p. 150–161, https://doi.org/10.1016/j.palaeo.2011.10.016.

Roe, G.H., Ding, Q., Battisti, D.S., Molnar, P., Clark, M.K., and Garzione, C.N., 2016, A modeling study of the response of Asian summertime climate to the largest geologic forcings of the past 50 Ma: Journal of Geophysical Research: Atmospheres, v. 121, p. 5453–5470, https://doi.org/10.1002/2015JD024370.

Su, T., Liu, Y.-S.C., Jacques, F.M.B., Huang, Y.-J., Xing, Y.-W., and Zhou, Z.-K., 2013, The intensification of the East Asian winter monsoon contributed to the disappearance of *Cedrus* (Pinaceae) in southwestern China: Quaternary Research, v. 80, p. 316–325, https://doi.org/10.1016/j.yqres.2013.07.001.

Printed in USA